State-associated changes in longitudinal $[^{18}F]$-PBR111 TSPO PET Imaging of psychosis patients : evidence for the accelerated ageing hypothesis?

Word count: 4121 words (excluding abstract, keywords, acknowledgements, conflict of interest, references, tables and figures)

Title: **State-associated changes in longitudinal [^{18}F]-PBR111 TSPO PET Imaging of psychosis patients: evidence for the accelerated ageing hypothesis?**

Authors: Livia De Picker MD*[1,2], Julie Ottoy MSc[3], Jeroen Verhaeghe PhD[3], Steven Deleye PhD[3], Leonie wyffels PhD[4], Erik Fransen PhD[5], Lauren Kosten MSc[3], Bernard Sabbe MD PhD[1,2], Violette Coppens PhD[1,2], Maarten Timmers MSc[6,7], Peter de Boer PhD[6], Luc Van Nueten MD[6], Ken Op De Beeck MD PhD[8], Herbert Oberacher PhD[9], Filip Vanhoenacker MD PhD[10], Sarah Ceyssens MD[4], Sigrid Stroobants MD PhD[4], Steven Staelens PhD[3], Manuel Morrens MD PhD[1,2]

1 Collaborative Antwerp Psychiatric Research Institute, Faculty of Medicine and Health Sciences, University of Antwerp, Antwerp, Belgium

2 University Department of Psychiatry, Campus Duffel, Duffel, Belgium

3 Molecular Imaging Center Antwerp, University of Antwerp, Antwerp, Belgium

4 Department of Nuclear Medicine, Antwerp University Hospital, Edegem, Belgium

5 StatUa Center for Statistics, University of Antwerp, Belgium

6 Janssen Research and Development, Janssen Pharmaceutica N.V., Beerse, Belgium

7 Reference Center for Biological Markers of Dementia (BIODEM), Institute Born-Bunge, University of Antwerp, Antwerp, Belgium

8 Medical Genetics Research Group, University of Antwerp, Antwerp, Belgium

9 Institute of Legal Medicine and Core Facility Metabolomics, Medical University of Innsbruck, Innsbruck, Austria

10 Department of Radiology, Sint-Maarten General Hospital, Mechelen, Belgium and Faculty of Medicine and Health Sciences, Universities of Antwerp and Ghent, Belgium

Location of work and address for reprints (Corresponding author*): Livia De Picker, Collaborative Antwerp Psychiatric Research Institute, Faculty of Medicine and Health Sciences, University of Antwerp Campus Drie Eiken, gebouw R D.R.327, Universiteitsplein 1, 2610 Antwerp, Belgium. Livia.depicker@gmail.com

ABSTRACT

Objective To determine whether state-associated changes in microglial activity, measured with translocator-protein positron emission tomography (TSPO PET), can be identified in psychosis patients through longitudinal evaluation of their regional tracer uptake over the clinical course from acute psychosis to post-treatment follow-up, and comparison to healthy controls. We also evaluated the relation between tracer uptake, clinical symptoms and peripheral immunological markers.

Method Second-generation radioligand [^{18}F]-PBR111 TSPO PET-CT was used for longitudinal dynamic imaging in 14 male psychosis patients and 17 male age-matched healthy control subjects. Patients were first scanned during an acute psychotic episode followed by a second scan after treatment. Prior genotyping of subjects for the rs6917 polymorphism distinguished high- and mixed-affinity binders. The main outcome was regional volume of distribution (V_T), representing TSPO binding. Plasma concentrations of CRP, cytokines and kynurenines were measured at each timepoint.

Results We found a significant three-way interaction between time of scan, age and cohort (cortical grey matter F6.50, p.020). Age-dependent differences in V_T existed between cohorts during the psychotic state, but not at follow-up. Patients' relative change in V_T over time correlated with age (cortical grey matter Pearson's r.574). PANSS positive subscale scores correlated with regional V_T during psychosis (cortical grey matter r.767). Plasma CRP and quinolinic acid were independently associated with lower V_T.

Conclusions We identified a differential age-dependent pattern of TSPO binding from psychosis to follow-up in our cohort of male psychosis patients. We recommend future

TSPO PET studies in psychosis patients to differentiate between clinical states and consider potential age-related effects.

Keywords:

Psychosis

Schizophrenia

Positron emission tomography

Microglia

Translocator protein

Kynurenines

Cytokines

Neuroinflammation

1. INTRODUCTION

A role for neuroinflammation in the pathophysiology of schizophrenia and psychosis has been implied by genome-wide association studies, postmortem and PET imaging studies, with a prominent role for the central nervous system's main immune regulators: the microglia (1). Exposure to inflammatory responses and/or genetically rooted excessive synapse pruning in the perinatal period (2) is thought to result in an activated or primed state of microglia in adulthood (1), leading to ongoing abnormal immune responses which drive psychotic episodes and cause an unfavorable illness course, with progressive loss of function and cumulative brain changes. Evidence from clinical studies suggests that psychotic exacerbations are accompanied by systemic immunological changes different from those seen in non-acute states, with patients during an acute psychotic event demonstrating increased IL-1β, IL-6, TGF-β and CD4/CD8 ratio which normalize after treatment (3, 4). We hypothesized the psychotic state to be accompanied with microglial activation in the brain, paralleling the state-associated changes observed in peripheral immunological markers.

In neuroinflammation, activated microglial cells increase their expression of the translocator protein 18kDa (TSPO) on the outer mitochondrial membrane. The detection of activated microglial cells is acquired in vivo through Positron Emission Tomography (PET) of the brain using a radioligand for TSPO. Previous studies of TSPO binding that were performed in relatively small samples of schizophrenia or psychosis patients in various stages of the illness, and using different tracers and methods of analysis have generated mixed results (3). In this study we evaluated central nervous system TSPO levels with fluoropropoxy-substituted-2-(6-chloro-2-phenyl)imidazo[1,2-a]pyridine-3-yl)-

N,N-diethylacetamide ([^{18}F]-PBR111), a novel second-generation tracer with high specific in vitro and in vivo binding to TSPO, which is best described by a 2-tissue compartment model with an additional vascular trapping component (5). Similar to other second-generation TSPO tracers, the use of [^{18}F]-PBR111 is complicated by the rs6971 polymorphism, requiring prior genotyping of study subjects to allow interpretation of tracer binding data.

We previously found the regional test-retest variability of [^{18}F]-PBR111 uptake in healthy controls from our sample to be 16-22%, which represents an acceptable standard for evaluating the longitudinal binding in these regions (5). To our knowledge, this is the first study to perform longitudinal TSPO PET imaging of acutely psychotic patients with follow-up examination post-treatment. Our primary aim is to evaluate if longitudinal changes of patients' regional [^{18}F]-PBR111 uptake differ from healthy age-matched controls. As secondary outcomes, we evaluate the relationship between [^{18}F]-PBR111 uptake and clinical symptoms or peripheral immunological markers, respectively.

2. MATERIALS AND METHODS

2.1 Subjects

We included 14 male patients with a diagnosis within the spectrum of primary psychotic disorders (DSM-5 #295.4-9, 298.8-9.; aged 18 to 50 years) who were admitted between January 2013 and December 2016 to the University Psychiatric Hospital Campus Duffel and the Psychiatric Hospital Multiversum (campus Boechout and Mortsel) for an acute

psychotic episode (first-episode psychosis or acute relapse; defined as total score ≥14 on the positive scale of the Positive and Negative Syndrome Scale (PANSS) + a score of ≥5 on one or a score of ≥4 on two of the "positive factor" PANSS items P1, P3, P5 or G9 (6, 7)). PANSS interviews were performed by a trained interviewer within one week prior to each PET scan, but not obtained for two subjects. All patients had been free of antipsychotic therapy for >4 weeks before hospitalization, after which medication was initiated based on clinical needs. Because benzodiazepines were found to have affinity for the TSPO receptor, no use of benzodiazepines was allowed for three times their half-life prior to each PET-scan.(8) A second cohort consisted of 17 male age-matched healthy controls without personal history of any primary psychiatric disorder nor family history of psychotic or bipolar disorders.

Main exclusion criteria were the use of any immunomodulating drugs within 21 days of participation; medical history of auto-immune disorders or other physical illness associated with abnormal immune changes within 14 days of participation and a positive test for alcohol or drugs of abuse, except cannabis or benzodiazepines (provided subjects did not meet DSM-5 criteria for substance use disorders within 3 months prior to the study).

Subjects underwent two 90-min dynamic [^{18}F]-PBR111 PET-scans at least 8 weeks apart at the same time of day. Patients were first scanned during the psychotic episode and again after ≥8 weeks of treatment in the absence of psychosis (PANSS positive scale total score ≤13 and ≤3 on items P1, P3, P5 or G9) - further indicated as “follow-up“ in this paper. In addition, subjects underwent MRI for evaluation of brain morphology within six months after PET imaging.

Approval for the study was obtained from the Committee for Medical Ethics of the University Hospital Antwerp (13/37/348) and of all participating hospitals. The project was registered under clinicaltrials.gov (NCT02009826). All participants provided informed consent.

2.2 Genotyping

Prior genotyping of subjects for the rs6971 polymorphism within the TSPO gene distinguished high- and mixed-affinity binders (HABs and MABs, respectively) while low-affinity binders were excluded. Following DNA extraction of whole venous blood samples collected at screening, we performed a PCR reaction using following primers: GAT-CTC-CTG-CTG-GTC-AGT-GG and TGC-AGA-AAG-CAC-AGG-ACA-CT. This reaction yields a PCR fragment surrounding the rs6971 SNP in the TSPO gene. The resulting fragments were purified using Calf Intestine Alkaline Phosphatase (Sigma-Aldrich, USA) and sanger sequenced using a Big Dye Terminator Cycle Sequencing kit (ThermoFisher, USA). Next, the reactions were loaded on an ABI 3130XL genetic analyzer. Resulting sanger traces were evaluated in CLC workbench version 5.7.1 (CLC Bio, Denmark).

2.3 Peripheral blood measurements

Non-fasting blood samples were acquired in a standardized manner at the same time of day and within one hour prior to each PET scan. Blood was drawn in EDTA and citrate containing tubes via a forearm vein, transferred to the laboratory (<5min) and stored at 4-8°C until centrifugation (<30min). Samples were centrifuged for 10min at 4°C and the resulting plasma aliquots were frozen immediately at -30°C until analysis.

Kynurenine pathway analytes Kynurenine (Kyn), Quinolinic Acid (QA) and Kynurenic Acid (KA) were measured in citrate plasma at the Institute of Legal Medicine and Core Facility Metabolomics (Medical University of Innsbruck, Austria) using a validated liquid chromatography–tandem mass spectrometry (LCMS) method of analysis (9).

Cytokines of interest were measured in duplicate in EDTA plasma by an electrochemiluminescence immunoassay technique developed by Mesoscale Discovery (Rockville, USA), according to the manufacturer's instructions. We used standardized kits V-PLEX Proinflammatory Panel 1 Human Kit (for detection of IL6, IL8 and TNFα) and V-PLEX Vascular Injury Panel 2 Human Kit (for CRP). Additionally, IL-1RA was detected using a custom 4-Spot Prototype Human IL-1RA kit. We calculated concentrations for each cytokine by fitting the sample signals on a 4-parametric logistic calibration curve. We excluded an individual assay if concentrations were below detection threshold in >50% of subjects, as well as all data points with an intra-assay coefficient of variation >15%. For all analyses, we prespecified the samples' processing order so samples belonging to the same subject were in the same batch, and each batch contained an equal distribution of patient and control samples. Quality control samples were added to each batch. Plasma sample data were not obtained in one control and three patients.

2.4 PET and MRI data acquisition and analysis

Procedures for acquisition and analysis of PET and MR images are described in Ottoy *et al* (10). In short, a 3-dimensional T1-weighted magnetization-prepared rapid gradient echo (MPRAGE) scan was performed on a Siemens Magnetom Aera 1.5T MR scanner (Erlangen, Germany), while PET data were acquired using a Siemens Biograph

mCT time-of-flight PET-scanner and recorded over 90 min following an intravenous bolus injection of 192±19MBq of [^{18}F]-PBR111.

A metabolite-corrected hybrid plasma input function was created from 5min continuous arterial blood sampling (Twilite, Swisstrace, Switzerland) complemented by 8 manual samples. A metabolite-corrected hybrid plasma input function was created from 5min continuous arterial blood sampling (Twilite, Swisstrace, Switzerland) complemented by 8 manual samples. Plasma-to-whole blood was lower in schizophrenia patients compared to healthy controls as shown earlier (5). The plasma free fraction did not differ significantly between clinical groups (Supplementary Figure 1, one-way ANOVA corrected for multiple comparisons via Tukey), and was not considered for V_T calculation (11).

Regional volume of distribution (V_T) was derived using a region-of-interest (ROI) based two-tissue compartmental analysis with an additional irreversible vascular trapping component. To account for progressive loss of whole brain volume and whole brain grey matter associated with schizophrenia(12), all TACs were corrected for partial volume effects based on the region-based geometric transfer matrix method (GTM as described by Rousset et al.) and a 5x5x5mm PET scanner resolution.(13) ROIs for this study were delineated based on automatic brain segmentation of the MRIs (PMOD Technologies Ltd., Zurich, Switzerland) and included total cortical grey matter (cortical GM), total cortical white matter (cortical WM), cerebellum, brainstem, cingulate cortex, thalamus, basal ganglia, amygdala and hippocampus. Interframe motion correction of the dynamic PET scans and PET-MRI co-registration were performed for each subject separately using PMOD v3.6 (PMOD Technologies Ltd., Zurich, Switzerland).

2.5 Statistical analysis

Baseline differences in clinical and demographic parameters between cohorts were examined by two-tailed independent t-tests for continuous variables and Pearson chi-square test for categorical variables. All data are presented as mean ± SD.

We performed a series of linear mixed model analyses, with regional V_T values as the dependent variables. The full model included subject number as random effect and genotype, cohort, time, age, age² (and their interactions) as fixed factors, which was simplified by stepwise backward elimination of the non-significant terms. Because a significant three-way interaction between time, age and cohort was observed in our primary model, we repeated this linear mixed model analysis after splitting the data from the patient cohort by time. The control cohort data were not split for time as we consider them to be part of the same sample, based on our earlier test-retest analysis. We also calculated differential scores representing the relative change in V_T from the first to second scan ($\Delta V_T=(V_{T1} - V_{T2}) / V_{T1}$) for each subject and used these as dependent variable in a linear regression analysis with age, cohort and their interaction as independent variables. Additionally, adjusted models with subject characteristics (smoking, cannabis use and BMI) and peripheral blood variables as covariates were tested. P-values were corrected for multiple testing (across 9 ROIs) using the The Benjamini-Hochberg implementation (14) of the False Discovery Rate (FDR) correction. An FDR adjusted p-value of .05 was used as cutoff for significance (significant p-values are indicated by *).

All statistical analyses were performed in JMP version 13, except for partial correlation analyses, which were done in IBM SPSS version 24. These latter analyses tested the association of V_T with symptom severity and peripheral immune markers, accounting for covariates age and genotype.

3. RESULTS

3.1 Subjects

Demographic information is presented in Table A. Three patients discontinued the study after the first scan. Data of 6 PET scans were excluded from analysis because of technical issues during arterial blood sampling (n=1 patient) or due to artefacts caused by subjects' head movement during 90 min PET imaging (n=3 patients and n=2 controls). This resulted in data for n= 11 patients and n=16 healthy controls available for analysis at the first scan point and n=10 patients and n=16 healthy controls at follow-up (10). Patients' baseline PANSS total scores, positive subscale and general psychopathology subscale scores were significantly higher than at follow-up.

***Table A**: Subject characteristics, raw outcome scores and PANSS interview scores*

	Controls (n=17)	**Patients (n=14)**	**Test statistic**	**Two-tailed p value**
Genotype	41,2% HAB	57,1% HAB	X^2 0.48	.491

	58,8% MAB	42.9% MAB			
Scan interval	19.9 ± 10.3 weeks	12.3 ± 4.6 weeks		T 2.27	.032
Age (y)	27.2 ± 5.5	32.2 ± 8.3		t -1.71	.098
Duration of illness (y)		5.2 ± 7.6 (n=9 DOI <5y)			
BMI	23.3 ± 1.8	25.5 ± 3.9		t -2.42	.023
Smoking	11.8%	78.6%		X^2 13.03	<.001
Cannabis use	5.9% occasional use	21.4% occasional use 28.6% regular use		X^2 9.18	.010
Antipsychotic use		90.9% at first scan 80% at follow-up			
	(average of both timepoints)	**First scan**	**Follow-up**		
V_T cortical GM	1.78 ± 0.64 HAB (n=7) 1.59 ± 0.46 MAB (n=10)	2.54 ± 1.11 HAB (n=6) 1.53 ± 0.31 MAB (n=5)	2.70 ± 0.83 HAB (n=6) 1.39 ± 0.20 MAB (n=4)		
V_T cortical WM	1.39 ± 0.33 HAB 1.37 ± 0.35 MAB	1.66 ± 0.53 HAB 1.36 ± 0.20 MAB	1.80 ± 0.41 HAB 1.30 ± 0.14 MAB		
V_T cerebellum	1.83 ± 0.69 HAB 1.66 ± 0.52 MAB	2.49 ± 0.79 HAB 1.52 ± 0.27 MAB	2.63 ± 0.91 HAB 1.53 ± 0.20 MAB		
V_T brainstem	2.21 ± 0.85 HAB 2.07 ± 0.48 MAB	3.14 ± 1.00 HAB 1.90 ± 0.45 MAB	3.38 ± 1.23 HAB 2.02 ± 0.59 MAB		
V_T cingulate	2.05 ± 0.69 HAB 1.76 ± 0.44 MAB	2.81 ± 1.17 HAB 1.73 ± 0.30 MAB	3.02 ± 0.96 HAB 1.67 ± 0.08 MAB		

V_T thalamus	2.41 ± 0.90 HAB 2.16 ± 0.53 MAB	3.23 ± 1.36 HAB 2.03 ± 0.41 MAB	3.55 ± 1.11 HAB 1.87 ± 0.24 MAB		
V_T basal ganglia	1.84 ± 0.56 HAB 1.67 ± 0.48 MAB	2.64 ± 0.94 HAB 1.55 ± 0.27 MAB	2.56 ± 0.68 HAB 1.45 ± 0.14 MAB		
V_T amygdala	2.21 ± 0.92 HAB 1.92 ± 0.43 MAB	3.27 ± 1.37 HAB 1.87 ± 0.32 MAB	3.20 ± 1.03 HAB 1.82 ± 0.20 MAB		
V_T hippocampus	2.30 ± 1.04 HAB 2.11 ± 0.51 MAB	3.28 ± 0.84 HAB 2.03 ± 0.41 MAB	3.23 ± 1.08 HAB 2.39 ± 0.86 MAB		
		First scan	**Follow-up**	**Matched pairs T-test** (df 7)	**Two-tailed p value**
PANSS interview scores	*Total*	75.3 ± 21.0	58.6 ± 12.0	t 4.7	.002
	Positive subscale	24.1 ± 5.4	9.6 ± 2.2	t 10.4	.001
	Negative subscale	16.7 ± 7.2	17.0 ± 8.2	t -0.3	.0.75
	General psychopathology subscale	34.5 ± 10.6	30.8 ± 5.2	t 3.5	.010

3.2 Patients with schizophrenia versus healthy controls

To model differences in V_T over time between the cohorts, allowing for effects of genotype and age, we fitted linear mixed models. Our primary linear mixed model (V_T = [SubjID] + genotype + cohort + time + cohort*time) could not demonstrate a significant difference in

the longitudinal change of V_T between patients and controls within any of the regions. Yet when a possible interaction effect with age was considered, we observed a significant three-way interaction between cohort, time and age, indicating that the difference in V_T between the cohorts varied depending on subjects' age, and that this relationship behaves differently across the two time points. Based on the graphical presentation, we further improved the fit of the model by operating a quadratic age effect (AICc 110 for the quadratic effect versus AICc 112.5 for the linear effect in cortical GM). The final model (V_T = [SubjID] + genotype + cohort + time + age + age² + cohort*time + cohort*age² + age²*time + cohort*time*age²) demonstrated a significant three-way interaction between cohort, time and age² in all regions (cortical GM F6.50, p.020; cfr. Figure A.1; Supplementary Table A.1). Duration of illness, cannabis use, smoking and BMI were not significant covariates.

To further evaluate the interaction between cohort, age and time, a second linear mixed model analysis was performed in which healthy control data were compared to data derived from patients during the psychotic episode. We again observed a significant interaction between age and cohort with a quadratic age effect (cortical GM cohort*age F18.92, p<.001; age² F16.99, p<.001; cfr. Figures A.2 and B; Supplementary Table A.2).

We subsequently performed a similar analysis using the data of patients at follow-up. Age was significant as a covariate, but there was no significant interaction between age and cohort. When adjusted for age and genotype, schizophrenia patients demonstrated slightly elevated V_Ts compared to healthy controls in most regions, yet only in the brainstem (F9.28, p.006), amygdala (F6.70, p.016) and hippocampus (F9.64, p.005) the

differences surpassed the FDR significance threshold (cfr. Figure A.3; Supplementary Table A.3).

Figure A: *Dot plot of F-values in final linear mixed models*

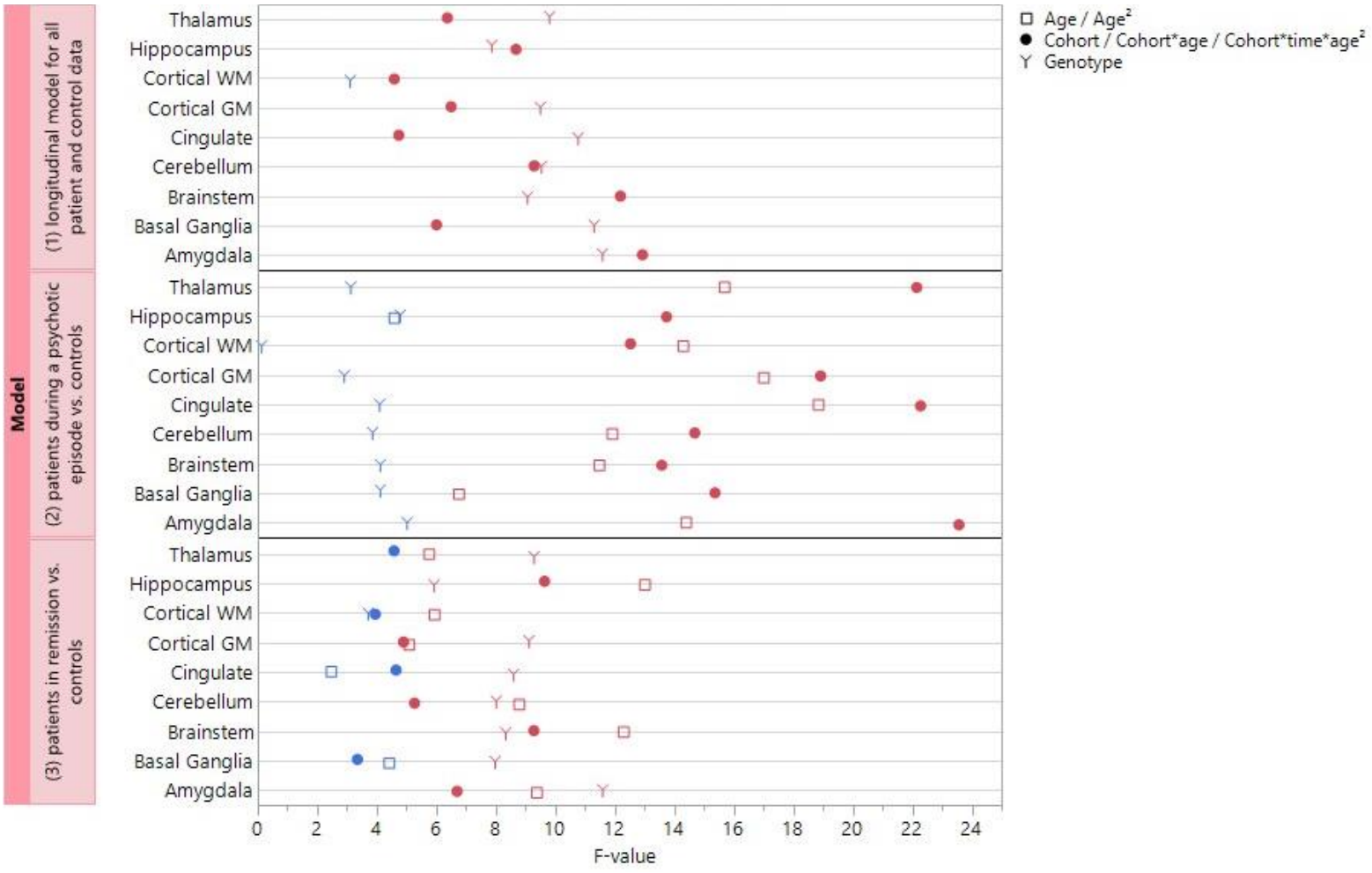

Legend: Dot plot of F-values for the main (or highest-order) terms in each final linear mixed model, per region of interest. Red symbols indicate significance level is attained under FDR correction, blue symbols indicate nonsignificant terms. Final linear mixed models include the following (terms shown in the graph are underlined):

*(1) longitudinal model for all patients and control data: V_T = [SubjID] + <u>genotype</u> + cohort + time + age + age² + cohort*time + cohort*age² + age²*time + <u>cohort*time*age²;</u> (2) patients during a psychotic episode vs. controls: V_T = [SubjID] + <u>genotype</u> + cohort + age + <u>age²</u> + <u>cohort*age</u>; (3) patients in remission vs. controls: V_T= [SubjID] + <u>genotype</u> + <u>cohort</u> + <u>age.</u> Detailed information on all F- and p-values in these models can be found in Supplementary Table A.*

***Figure B**: Relationship between age and V_T in cortical grey matter*

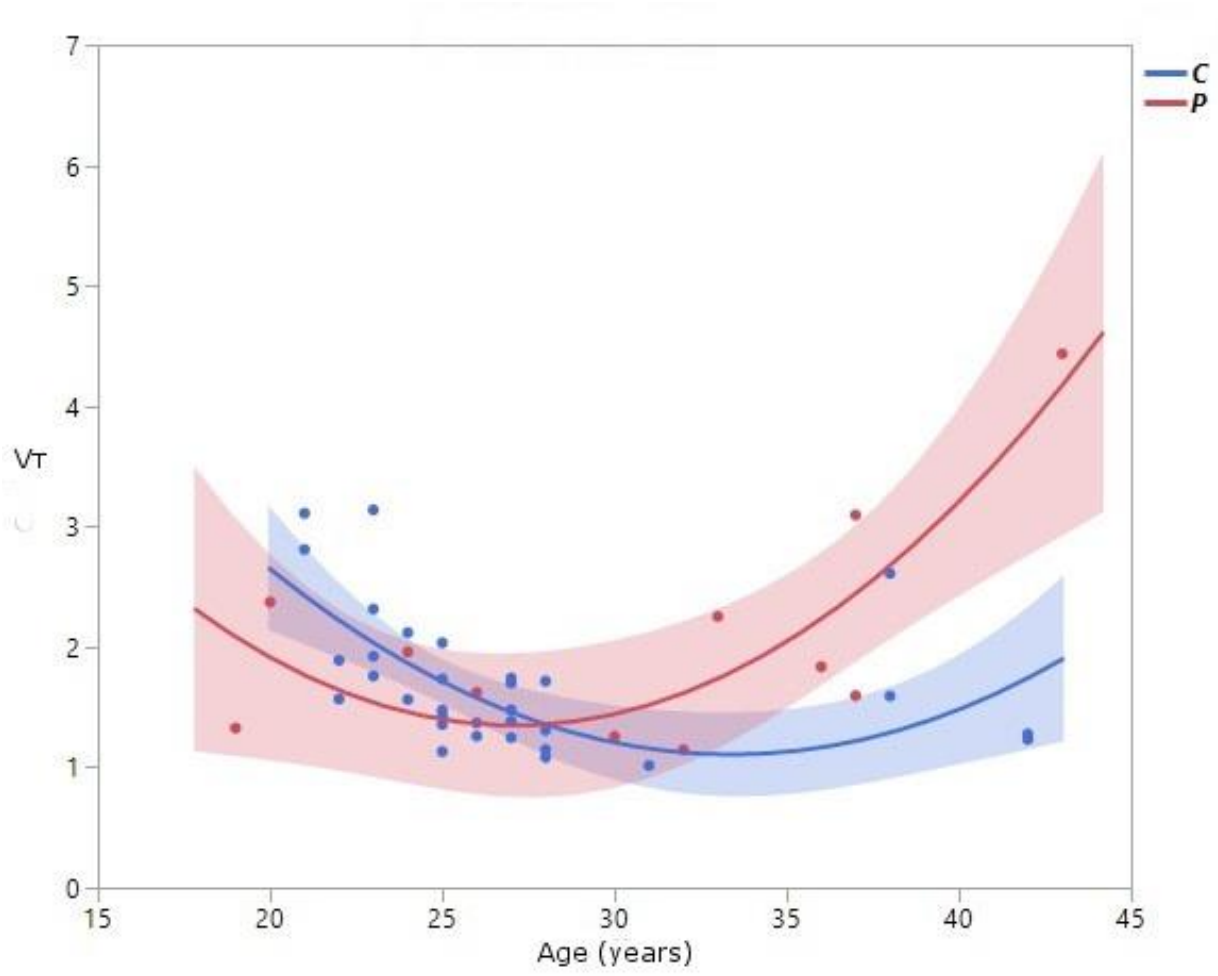

Legend: quadratic relationship between age (in years) and V_T in cortical grey matter of patients during a psychotic episode (P; n=11) versus controls (C; n=17 subjects, 32 data points).

Finally, strong correlations between ΔV_T and age were found in the patient group in all regions, with the highest correlations in the hippocampus (r.901, p.002), brainstem (r.827, p.011) and amygdala (r.784, p.021), while in the control group no relevant correlations with age (|r|<0.3) in all regions) were found (cfr. Figure C, Supplementary Table B.1). Regression analysis (ΔVT = age + cohort + age*cohort) confirmed medium effect sizes

for the interaction term in the brainstem (η² .243, p.016), cerebellum (η² .216, p.025), amygdala (η² .210, p.021), hippocampus (η² .196, p.029) and cortical gray matter (η² .137, p.086), yet these did not reach FDR significance level in any region.

Figure C: *Relationship between age and ΔV_T scores in the hippocampal region*

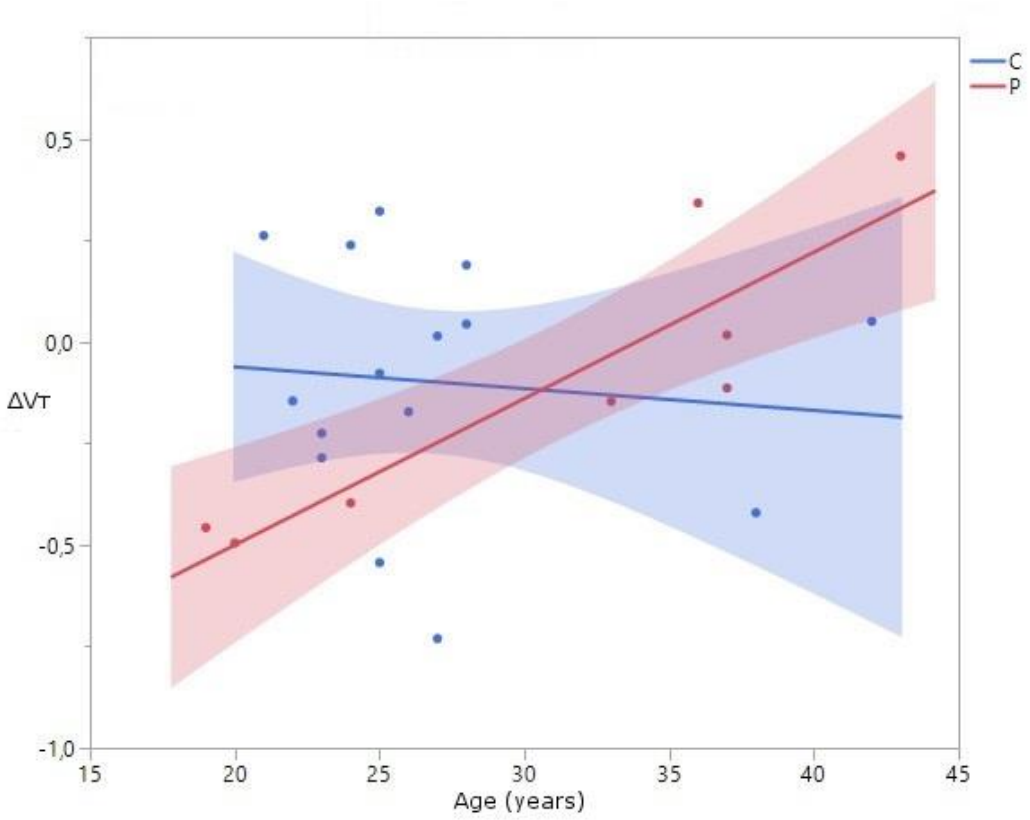

Legend: Linear relationship between age and ΔV_T scores (=relative change in V_T between the first and second scan) of patients (P; n=8) and controls (C; n=15) in the hippocampal region.

3.3 Relation with clinical symptomatology and peripheral immune markers

Peripheral immune markers (CRP, TNFα, IL1RA, IL6, IL8, KA, QA, QA/KA ratio, KA/Kyn ratio) were measured together with each PET scan to evaluate their association with TSPO uptake. There were no major group or longitudinal differences in plasma concentrations except for a lower concentration of KA in patients (linear mixed model analysis after adjusting for BMI and age, cohort F13.7, p.001). The QA/KA ratio increased significantly between the first and follow-up scans in patients but not in controls (cohort*time F26.7, p<.001).

We analyzed partial correlations between regional V_T and PANSS subscale scores or peripheral immune markers, accounting for age and genotype. For patients during a psychotic episode, we identified strong positive correlations with scores on the PANSS positive subscale in all regions of interest (cortical GM r.767, p.026), but not with other subscales (cfr. Supplementary Table B.2). The regional V_T of patients during a psychotic episode also correlated positively with QA/KA ratio (cortical GM r.873, p.010) and negatively with KA concentrations (cortical GM r-1.000, p<.001). Regional V_Ts of patients at follow-up correlated negatively with KA concentrations (cortical GM r-1.000, p<.001) and QA concentrations (except for amygdala region, cortical GM r-1.000, p<.001). Finally, in healthy controls, [^{18}F]-PBR111 uptake correlated negatively with CRP concentrations (cortical GM r-.530, p.005) as well as IL8 concentrations (cortical GM r-.482, p.013).

Addition of peripheral immune markers QA*cohort and CRP as covariates (defined by stepwise comparison of different linear mixed models) improved the fit of our earlier linear mixed model significantly (AICc 80.8 for cortical GM). (cfr. Supplementary Table C).

4. Discussion

4.1 Interpretation of Findings

The outcomes of our study point towards a differential pattern of tracer uptake from psychosis to post-treatment follow-up, mediated by patients' age. Older patients were more likely to demonstrate higher TSPO binding in the psychotic state and an associated decrease at follow-up, whereas younger patients exhibited a reverse pattern with lower uptake in the acute phase followed by a relative increase (cfr. Figure D).

***Figure D**: Patients' change in TSPO binding over time in the hippocampal region*

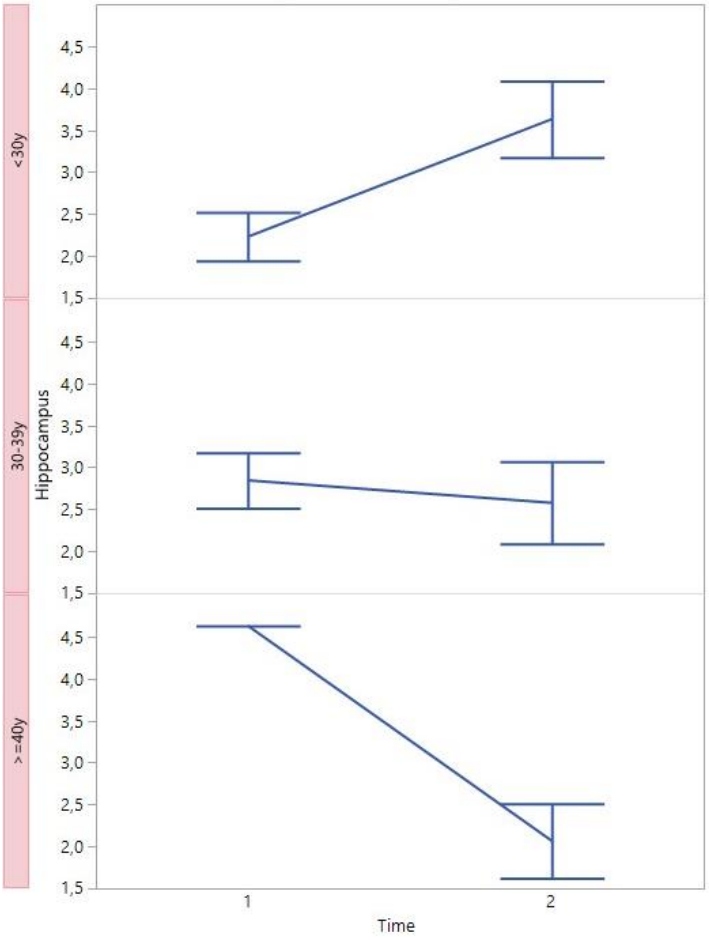

Legend: Patients' change in TSPO binding over time in the hippocampal region for three age categories (<30y n=5; 30-39y n=6, ≥40y n=2). Time 1 = first scan during acute psychotic state; Time 2 = Post-treatment follow-up. Data points represent mean ± SE.

Previous TSPO studies in psychosis patients (summarized in De Picker *et al* 2017) have been heterogeneous in their choice of tracer, kinetic model, outcome measure and patient population, leading to mixed results which have been difficult to interpret. A recent meta-analysis of TSPO PET studies with second generation tracers (n=5 (15-19)) by Plavén-Sigray *et al* (online preprint prior to peer-review) concluded the evidence in favor of a relative decrease in tracer uptake in psychosis patients compared to healthy controls largely outweighs the evidence for a relative increase, however age was not included as a covariate (20). Compared to these studies, the patients in our sample were significantly older than those from Coughlin *et al* (t3.26, df17, p.004) and significantly younger than those from Kenk *et al* (t2.48, df24.3, p.020) and Bloomfield *et al* (t4.25, df21.8, p<.001), who found a significant correlation between age and [11C]PBR28 VT in total gray matter (15, 16, 18). Autoradiographic studies have reported both higher (21) and lower (22) TSPO binding in patients. Our data suggest that, depending on the clinical state and the age of the patient at the time of the investigation, both hypotheses may be true.

Our data seem to indicate an age-related increase in TSPO binding in psychotic patients which is different from or accelerated compared to healthy controls. Such age-related increases in microglia and TSPO have been reported in animal, human and postmortem studies and are usually considered consequences of age-related oxidative damage to DNA and accumulation of glycated proteins, causing a compensatory upregulation of microglial 'housekeeping' functions. We however did not find any significant effect of duration of illness on TSPO uptake. Our findings in psychosis patients may therefore reflect the premature onset of physiological changes associated with normal aging. Moreover, a similar accelerated ageing trajectory has been observed in schizophrenia

patients related to age-related decreases in neuroplasticity (23, 24). Increased TSPO binding in older patients could therefore also signify the compensatory effects of a microglial system struggling to keep up amidst failing neuroplasticity. Interestingly, these age-related cumulative changes may offer a microanatomical explanation for the progressive anatomical abnormalities of brain structure recorded in longitudinal studies of psychosis patients, including the characteristic enlarged ventricle size and reductions in grey matter volume, whole-brain volume, and white matter anisotropy (25).

Besides age, we identified peripheral immune markers from two separate immunological pathways as independent predictors of TSPO binding. The acute phase protein CRP correlated inversely with tracer uptake in controls, while kynurenine pathway metabolites such as quinolinic acid but also kynurenic acid were negatively associated with uptake uniquely in patients. To our knowledge, no prior studies have investigated the effects of kynurenines or CRP on TSPO binding in psychosis patients. Coughlin *et al* did not identify any significant effect of plasma IL1β, IFNγ, IL-10, IL-6 and TNF-α concentrations on [^{11}C]DPA-713 uptake in recent-onset patients (16), nor did Di Biase *et al* for serum IL-1β, TNF-α and IL-6 on [^{11}C]PK11195 uptake in ultra-high risk, recent-onset and chronic patient groups (26). Several meta-analyses have demonstrated increases in pro-inflammatory markers, such as cytokines and CRP, in CSF and plasma of patients suffering from psychotic illness (4, 27, 28). In the brain, microglia and astrocytes are the key players involved in the immune response (29). Therefore, increases in numbers or activity of these cells have been hypothesized to accompany peripheral pro-inflammatory changes. Interestingly, we observed an inverse correlation between CRP and TSPO binding in healthy controls. Based on the hypothesis that systemic inflammation can

trigger microglial activation, one would expect the opposite. However, while the relationship between systemic immune responses and the brain remains poorly understood (30), it was recently suggested that systemic pro-inflammatory signals provoke a compensatory decrease in TSPO signal in the brain (31, 32).

Finally, we observed significant correlations between PANSS positive subscale scores and the tracer uptake of patients during a psychotic episode, though only when corrected for age and genotype. This suggests that during an acute episode, the severity of the psychotic symptoms mediates the amount of TSPO expression, although our study design did not allow us to further evaluate this hypothesis. In their meta-analysis, Plavén-Sigray *et al* found little to no evidence for a correlation between regional V_T and PANSS scores. In comparison, the PANSS positive scores in our sample were significantly higher (24.1±5.4 at the time of the first scan in our patient sample versus 18,2±4,2 pooled mean of Plavén-Sigray *et al*; t3.47, df11.3, p.004) (20).

4.2 Limitations

Whereas our sample sizes are in line with those of previous studies, our a priori power was decreased due to the less than perfect test-retest reliability of the tracer (10). Missing data and exclusions related to technical difficulties related to the scanning protocol caused additional loss of power. We therefore preferred methods of analyses which are less affected by missing data, such as linear mixed models. Analyses which were more vulnerable to missing data were the correlation analyses stratified by subgroups and the regression model for ΔV_T. V_T values were derived from a metabolite corrected plasma input function but V_T was not corrected for plasma free fraction as fp values cannot be

accurately measured through ultrafiltration. However, no significant differences in fp were found between the different groups. Further technical challenges related to this study are discussed in Ottoy *et al* (10). It has been our concern that the complexity and invasiveness of the scanning protocol combined with the restrictive inclusion criteria (including a requirement for patients not to use benzodiazepines prior to the scan) arguably represented a significant cause of missing or excluded data and non-response bias. Although patients in our sample demonstrated symptom severity scores in the same range or higher than previous TSPO studies, less demanding scanning protocols are clearly needed particularly for patient groups with a high symptomatic burden and/or during an acute psychotic episode.

Our study was not a priori designed to examine age-related effects and included only two patients older than 40 years of age. These results therefore require cautious interpretation and need to be replicated in studies specifically designed to compare different age groups of psychosis patients. Furthermore, the mean age of HAB and MAB subjects differed significantly in controls (HAB mean 29.6±1.35y; MAB 25.5±1.13y; t2.31, p.030), but not in patients (t0.42). We therefore cannot exclude that the age-dependent increase in V_T observed in controls is caused by a genotype imbalance. The effect of age on TSPO expression in healthy human brains as examined by [^{11}C]-PK11195 (33-36) or by newer TSPO radioligands [^{11}C]-vinpocentine, [^{11}C]-DAA1106 and [^{18}F]-FEPPA (37-39) has generated mixed results.

Almost all patients in our study were medicated during the scans and so we cannot rule out changes in the patient group may be due to antipsychotic treatment. However, a

recent [3H]PBR28 autoradiography study in rats demonstrated haloperidol does not affect microglial cell density, morphology or TSPO expression.(40) Another potential confounder could be the higher proportion of smokers among schizophrenia patients compared to healthy controls. Although smoking status was not found to be a significant covariate in our analysis, one study found whole brain standardized uptake values of [11C]-DAA1106 in smokers to be significantly lower compared to non-smokers.(40) Moreover, for statistical as well as safety reasons, our study only included male subjects and our findings may therefore not apply to female psychosis patients.

Finally, the direct biological relationship between microglia and TSPO binding in vivo is still not fully understood. Not only microglial cells, but also astrocytes as well as endothelial cells have been revealed as cellular sources of TSPO expression in CNS pathology (41). Even if changes in TSPO tracer uptake truly reflect altered microglial activation, PET images cannot differentiate between the various morphological and functional states which activated microglial cells can display, ranging from pro- to anti-inflammatory. Contrary to the widespread notion that increased TSPO expression is a hallmark of pro-inflammatory states, recent in vitro data suggests that pro-inflammatory macrophages may show reduced TSPO expression (42). Interpretation of altered TSPO binding is therefore complex, as it may reflect both a protective response or a damaging neuroinflammatory process and will require accompanying neuropathological studies.

4.3 Conclusions and recommendations

In this paper we provide, to our knowledge, the first longitudinal evidence that TSPO binding of male psychosis patients from acute psychosis to post-treatment remission

changes could be dependent on patients' age. We also show that TSPO binding in patients during a psychotic episode increases with their age and the severity of the psychotic symptoms. Peripheral concentrations of acute phase protein CRP and kynurenine pathway metabolite quinolinic acid correlated negatively with TSPO binding. We strongly recommend investing in more longitudinal studies, while considering the need for a larger sample size due to less than ideal tracer reliability. Secondly, we advocate study designs that allow to differentiate patients in different clinical states and assess potential age-related effects.

Conflict of interest

This study was in part funded by research grants from the Flanders' Agency for Innovation by Science and Technology (IWT) and Janssen Research and Development, a division of Janssen Pharmaceutica N.V. Neither funding body was responsible for the design, collection and analysis of data or the decision to publish. Authors M. Timmers, P. de Boer and L. van Nueten are employees of Janssen Pharmaceutica N.V. and the findings of this research may affect future research lines within the company.

Acknowledgements

The authors are thankful to Marleen Cauchie, Annemie Van Eetveldt, Caroline Berghmans and Philippe Joye for support with the PET scanning procedures. The authors are equally thankful to Ingrid Vanderplas, Silke Apers, Liesbet Claes and Sarah Debruyne for their support with all patient-related procedures. Finally, we would like to express our gratitude to all the participants of this study.

References

1. Monji A, Kato T, Kanba S. Cytokines and schizophrenia: Microglia hypothesis of schizophrenia. *Psychiatry and clinical neurosciences* 2009;**63**:257-65.
2. Sekar A, Bialas AR, de Rivera H, Davis A, Hammond TR, Kamitaki N et al. Schizophrenia risk from complex variation of complement component 4. *Nature* 2016;**530**:177-83.
3. De Picker LJ, Morrens M, Chance SA, Boche D. Microglia and Brain Plasticity in Acute Psychosis and Schizophrenia Illness Course: A Meta-Review. *Frontiers in psychiatry* 2017;**8**:238.
4. Miller BJ, Buckley P, Seabolt W, Mellor A, Kirkpatrick B. Meta-analysis of cytokine alterations in schizophrenia: clinical status and antipsychotic effects. *Biological psychiatry* 2011;**70**:663-71.
5. Ottoy J, De Picker L, Verhaeghe J, Deleye S, Wyffels L, Kosten L et al. (18)F-PBR111 PET Imaging in Healthy Controls and Schizophrenia: Test-Retest Reproducibility and Quantification

of Neuroinflammation. *Journal of nuclear medicine : official publication, Society of Nuclear Medicine* 2018;**59**:1267-74.
6. Wallwork RS, Fortgang R, Hashimoto R, Weinberger DR, Dickinson D. Searching for a consensus five-factor model of the Positive and Negative Syndrome Scale for schizophrenia. *Schizophrenia research* 2012;**137**:246-50.
7. Kay SR, Fiszbein A, Opler LA. The positive and negative syndrome scale (PANSS) for schizophrenia. *Schizophrenia bulletin* 1987;**13**:261-76.
8. Doorduin J, de Vries EF, Willemsen AT, de Groot JC, Dierckx RA, Klein HC. Neuroinflammation in schizophrenia-related psychosis: a PET study. *Journal of nuclear medicine : official publication, Society of Nuclear Medicine* 2009;**50**:1801-7.
9. Arnhard K, Pitterl F, Sperner-Unterweger B, Fuchs D, Koal T, Oberacher H. A validated liquid chromatography-high resolution-tandem mass spectrometry method for the simultaneous quantitation of tryptophan, kynurenine, kynurenic acid, and quinolinic acid in human plasma. *Electrophoresis* doi:10.1002/elps.201700400.
10. Ottoy J, De Picker L, Verhaeghe J, Deleye S, Wyffels L, Kosten L et al. [(18)F]PBR111 PET Imaging in Healthy Controls and Schizophrenia: Test - Retest Reproducibility and Quantification of Neuroinflammation. *Journal of nuclear medicine : official publication, Society of Nuclear Medicine* doi:10.2967/jnumed.117.203315.
11. Guo Q, Colasanti A, Owen DR, Onega M, Kamalakaran A, Bennacef I et al. Quantification of the specific translocator protein signal of 18F-PBR111 in healthy humans: a genetic polymorphism effect on in vivo binding. *Journal of nuclear medicine : official publication, Society of Nuclear Medicine* 2013;**54**:1915-23.
12. Harrison PJ, Freemantle N, Geddes JR. Meta-analysis of brain weight in schizophrenia. *Schizophrenia research* 2003;**64**:25-34.
13. Rousset OG, Ma Y, Evans AC. Correction for partial volume effects in PET: principle and validation. *Journal of nuclear medicine : official publication, Society of Nuclear Medicine* 1998;**39**:904-11.
14. Benjamini Y, Hochberg Y. Controlling the false discovery rate: a practical and powerful approach to multiple testing. *Journal of the Royal Statistical Society, Series B* 1995;**57**:289-300.
15. Bloomfield PS, Selvaraj S, Veronese M, Rizzo G, Bertoldo A, Owen DR et al. Microglial Activity in People at Ultra High Risk of Psychosis and in Schizophrenia: An [(11)C]PBR28 PET Brain Imaging Study. *The American journal of psychiatry* 2016;**173**:44-52.
16. Coughlin JM, Wang Y, Ambinder EB, Ward RE, Minn I, Vranesic M et al. In vivo markers of inflammatory response in recent-onset schizophrenia: a combined study using [(11)C]DPA-713 PET and analysis of CSF and plasma. *Translational psychiatry* 2016;**6**:e777.
17. Hafizi S, Tseng HH, Rao N, Selvanathan T, Kenk M, Bazinet RP et al. Imaging Microglial Activation in Untreated First-Episode Psychosis: A PET Study With [18F]FEPPA. *The American journal of psychiatry* 2017;**174**:118-24.
18. Kenk M, Selvanathan T, Rao N, Suridjan I, Rusjan P, Remington G et al. Imaging neuroinflammation in gray and white matter in schizophrenia: an in-vivo PET study with [18F]-FEPPA. *Schizophrenia bulletin* 2015;**41**:85-93.
19. Collste K, Plaven-Sigray P, Fatouros-Bergman H, Victorsson P, Schain M, Forsberg A et al. Lower levels of the glial cell marker TSPO in drug-naive first-episode psychosis patients as measured using PET and [(11)C]PBR28. *Molecular psychiatry* 2017;**22**:850-6.

20. Plavén-Sigray P, Matheson GJ, Collste K, Ashok AH, Coughlin JM, Howes OD et al. PET studies of the glial cell marker TSPO in psychosis patients - a meta-analysis using individual participant data. *BioRxiv preprint* Published online Dec 5, 2017.
21. Kreisl WC, Fujita M, Fujimura Y, Kimura N, Jenko KJ, Kannan P et al. Comparison of [(11)C]-(R)-PK 11195 and [(11)C]PBR28, two radioligands for translocator protein (18 kDa) in human and monkey: Implications for positron emission tomographic imaging of this inflammation biomarker. *NeuroImage* 2010;**49**:2924-32.
22. Kurumaji A, Wakai T, Toru M. Decreases in peripheral-type benzodiazepine receptors in postmortem brains of chronic schizophrenics. *Journal of neural transmission* 1997;**104**:1361-70.
23. Green MJ, Matheson SL, Shepherd A, Weickert CS, Carr VJ. Brain-derived neurotrophic factor levels in schizophrenia: a systematic review with meta-analysis. *Molecular psychiatry* 2011;**16**:960-72.
24. Parkhurst CN, Yang G, Ninan I, Savas JN, Yates JR, 3rd, Lafaille JJ et al. Microglia promote learning-dependent synapse formation through brain-derived neurotrophic factor. *Cell* 2013;**155**:1596-609.
25. Bakhshi K, Chance SA. The neuropathology of schizophrenia: A selective review of past studies and emerging themes in brain structure and cytoarchitecture. *Neuroscience* 2015;**303**:82-102.
26. Di Biase MA, Zalesky A, O'Keefe G, Laskaris L, Baune BT, Weickert CS et al. PET imaging of putative microglial activation in individuals at ultra-high risk for psychosis, recently diagnosed and chronically ill with schizophrenia. *Translational psychiatry* 2017;**7**:e1225.
27. Upthegrove R, Manzanares-Teson N, Barnes NM. Cytokine function in medication-naive first episode psychosis: a systematic review and meta-analysis. *Schizophrenia research* 2014;**155**:101-8.
28. Miller BJ, Culpepper N, Rapaport MH. C-reactive protein levels in schizophrenia: a review and meta-analysis. *Clinical schizophrenia & related psychoses* 2014;**7**:223-30.
29. Venneti S, Lopresti BJ, Wiley CA. Molecular imaging of microglia/macrophages in the brain. *Glia* 2013;**61**:10-23.
30. Perry VH. Stress primes microglia to the presence of systemic inflammation: implications for environmental influences on the brain. *Brain, behavior, and immunity* 2007;**21**:45-6.
31. Notter T, Coughlin JM, Gschwind T, Weber-Stadlbauer U, Wang Y, Kassiou M et al. Translational evaluation of translocator protein as a marker of neuroinflammation in schizophrenia. *Molecular psychiatry* 2018;**23**:323-34.
32. Forsberg A, Cervenka S, Jonsson Fagerlund M, Rasmussen LS, Zetterberg H, Erlandsson Harris H et al. The immune response of the human brain to abdominal surgery. *Annals of neurology* 2017;**81**:572-82.
33. Cagnin A, Brooks DJ, Kennedy AM, Gunn RN, Myers R, Turkheimer FE et al. In-vivo measurement of activated microglia in dementia. *Lancet* 2001;**358**:461-7.
34. Debruyne JC, Versijpt J, Van Laere KJ, De Vos F, Keppens J, Strijckmans K et al. PET visualization of microglia in multiple sclerosis patients using [11C]PK11195. *European journal of neurology* 2003;**10**:257-64.
35. Kumar A, Muzik O, Shandal V, Chugani D, Chakraborty P, Chugani HT. Evaluation of age-related changes in translocator protein (TSPO) in human brain using (11)C-[R]-PK11195 PET. *Journal of neuroinflammation* 2012;**9**:232.

36. Schuitemaker A, van der Doef TF, Boellaard R, van der Flier WM, Yaqub M, Windhorst AD et al. Microglial activation in healthy aging. *Neurobiology of aging* 2012;**33**:1067-72.
37. Suridjan I, Rusjan PM, Voineskos AN, Selvanathan T, Setiawan E, Strafella AP et al. Neuroinflammation in healthy aging: a PET study using a novel Translocator Protein 18kDa (TSPO) radioligand, [(18)F]-FEPPA. *NeuroImage* 2014;**84**:868-75.
38. Yasuno F, Ota M, Kosaka J, Ito H, Higuchi M, Doronbekov TK et al. Increased binding of peripheral benzodiazepine receptor in Alzheimer's disease measured by positron emission tomography with [11C]DAA1106. *Biological psychiatry* 2008;**64**:835-41.
39. Gulyas B, Vas A, Toth M, Takano A, Varrone A, Cselenyi Z et al. Age and disease related changes in the translocator protein (TSPO) system in the human brain: positron emission tomography measurements with [11C]vinpocetine. *NeuroImage* 2011;**56**:1111-21.
40. Bloomfield PS, Bonsall D, Wells L, Dormann D, Howes O, Paola V. The effects of haloperidol on microglial morphology and translocator protein levels: An in vivo study in rats using an automated cell evaluation pipeline. *Journal of psychopharmacology (Oxford, England)* 2018:269881118788830.
41. Cosenza-Nashat M, Zhao ML, Suh HS, Morgan J, Natividad R, Morgello S et al. Expression of the translocator protein of 18 kDa by microglia, macrophages and astrocytes based on immunohistochemical localization in abnormal human brain. *Neuropathology and applied neurobiology* 2009;**35**:306-28.
42. Narayan N, Mandhair H, Smyth E, Dakin SG, Kiriakidis S, Wells L et al. The macrophage marker translocator protein (TSPO) is down-regulated on pro-inflammatory 'M1' human macrophages. *PloS one* 2017;**12**:e0185767.

Article: State-associated changes in longitudinal [18F]-PBR111 TSPO PET Imaging of psychosis patients: evidence for the accelerated ageing hypothesis?

SUPPLEMENTARY INFORMATION

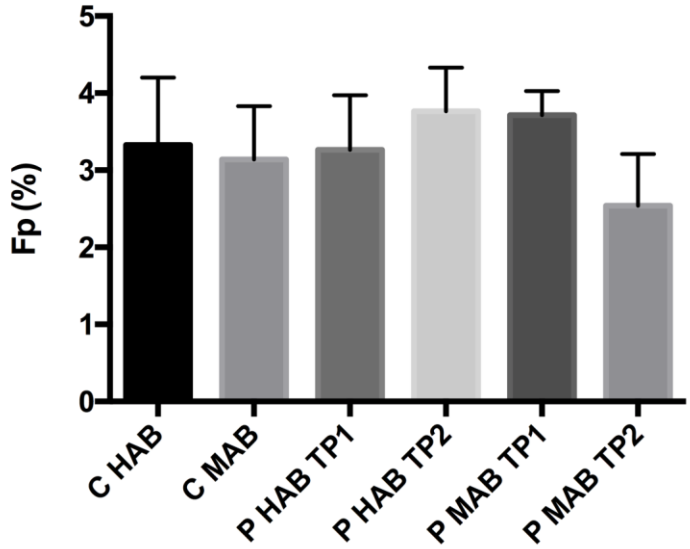

Supplementary Figure 1: Plasma free fraction (Fp%) for the different study groups (mean 3.27 ± 0.75%). C= controls; P= patients; TP1= first scan, TP2= follow-up scan.

Supplementary Table A: Details of the final longitudinal linear mixed models for

(1) all patient and control data.

(2) patients during a psychotic episode vs. controls;

(3) patients in remission vs. controls.

(1) Longitudinal model for all patients and control data	**V_T = [SubjID] + genotype + cohort + time + age + age² + cohort*time + cohort*age² + age²*time + cohort*time*age²**		
Region	*Term*	*F ratio (effect size)*	*p*
Cortical GM	Cohort*time*age² Genotype	6.50 9.50	.020* .005*
Cortical WM	Cohort*time*age² Genotype	4.59 3.11	.044* .090

Cerebellum	Cohort*time*age²	9.29	.006*
	Genotype	9.54	.005*
Brainstem	Cohort*time*age²	12.19	.002*
	Genotype	9.07	.006*
Cingulate	Cohort*time*age²	4.74	.042*
	Genotype	10.77	.003*
Thalamus	Cohort*time*age²	6.37	.021*
	Genotype	9.81	.005*
Basal Ganglia	Cohort*time*age²	6.01	.024*
	Genotype	11.31	.003*
Amygdala	Cohort*time*age²	12.93	.002*
	Genotype	11.59	.003*
Hippocampus	Cohort*time*age²	8.68	.008*
	Genotype	7.87	.010*
(2) Patients during a psychotic episode vs. controls	**V_T = [SubjID] + genotype + cohort + age + age² + cohort*age**		
Region	*Term*	*F*	*p*
Cortical GM	Cohort*age	18.92	<.001*
	Age²	16.99	<.001*
	Genotype	2.91	.102
Cortical WM	Cohort*age	12.53	.002*
	Age²	14.28	<.001*
	Genotype	0.13	.726

Cerebellum	Cohort*age Age² Genotype	14.69 11.90 3.86	<.001* .002* .062
Brainstem	Cohort*age Age² Genotype	13.58 11.46 4.12	.001* .002* .055
Cingulate	Cohort*age Age² Genotype	22.28 18.83 4.10	<.001* <.001* .055
Thalamus	Cohort*age Age² Genotype	22.15 15.67 3.13	<.001* <.001* .091
Basal Ganglia	Cohort*age Age² Genotype	15.37 6.74 4.12	<.001* .016* .055
Amygdala	Cohort*age Age² Genotype	23.57 14.38 5.02	<.001* <.001* .036
Hippocampus	Cohort*age Age² Genotype	13.74 4.57 4.79	.001* .043 .040
(3) Patients in remission vs. controls	**V_T= [SubjID] + genotype + cohort + age**		
Region	*Term*	*F*	*p*

Cortical GM	Cohort	4.90	.037*
	Genotype	9.12	.006*
	Age	5.07	.034*
Cortical WM	Cohort	3.95	.057
	Genotype	3.71	.066
	Age	5.92	.022*
Cerebellum	Cohort	5.27	.031*
	Genotype	8.02	.010*
	Age	8.77	.007*
Brainstem	Cohort	9.28	.006*
	Genotype	8.34	.009*
	Age	12.28	.002*
Cingulate	Cohort	4.65	.042
	Genotype	8.60	.008*
	Age	2.45	.132
Thalamus	Cohort	4.58	.043
	Genotype	9.29	.006*
	Age	5.74	.025*
Basal Ganglia	Cohort	3.35	.080
	Genotype	7.98	.010*
	Age	4.40	.047
Amygdala	Cohort	6.70	.016*
	Genotype	11.06	.003*
	Age	9.36	.006*

Hippocampus	Cohort Genotype Age	9.64 5.93 12.99	.005* .023* .001*

Supplementary Table B: Details of correlation analyses in patients.
(1) correlation analysis between relative change in V_T over time and age;
(2) partial correlation analysis between V_T during a psychotic episode and PANSS positive subscale scores (corrected for age and genotype)

	(1) ΔV_T versus age		**(2) V_T during psychotic episode versus PANSS positive subscale**	
	r	**P (two-tailed)**	**r**	**P (two-tailed)**
Cortical GM	.574	.136	.767	.026*
Cortical WM	.617	.103	.647	.083
Cerebellum	.724	.042	.900	.002*
Brainstem	.827	.011*	.778	.023*
Cingulate	.499	.208	.847	.008*
Thalamus	.604	.113	.789	.020*
Basal Ganglia	.562	.148	.869	.005*
Amygdala	.784	.021	.812	.001*
Hippocampus	.901	.002*	1.00	<.001*

Supplementary Table C: Details of the final longitudinal linear mixed model with peripheral immune markers as covariates

	V_T = [SubjID] + genotype + cohort + time + age + age² + cohort*time + cohort*age² + age²*time + cohort*time*age² + CRP + QA + QA*cohort		
Region	*Term*	*F*	*p*
Cortical GM	Cohort*time*age²	13.55	.002*
	Genotype	1.40	.252
	CRP	13.34	.001*
	QA*cohort	13.34	.001*
Cortical WM	Cohort*time*age²	6.85	.018*
	Genotype	0.24	.633
	CRP	14.60	.001*
	QA*cohort	4.79	.037
Cerebellum	Cohort*time*age²	12.48	.003*
	Genotype	2.50	.130
	CRP	8.42	.008*
	QA*cohort	4.73	.038
Brainstem	Cohort*time*age²	16.85	<.001*
	Genotype	1.68	.211
	CRP	10.50	.003*
	QA*cohort	4.82	.036
Cingulate	Cohort*time*age²	10.80	.005*
	Genotype	2.39	.139

	CRP	10.23	.004*
	QA*cohort	13.85	<.001*
Thalamus	Cohort*time*age²	11.33	.004*
	Genotype	1.56	.228
	CRP	10.77	.004*
	QA*cohort	10.37	.003*
Basal Ganglia	Cohort*time*age²	5.99	.030
	Genotype	1.18	.294
	CRP	6.90	.016*
	QA*cohort	2.64	.115
Amygdala	Cohort*time*age²	12.39	.004*
	Genotype	1.91	.187
	CRP	10.88	.004*
	QA*cohort	5.67	.024*
Hippocampus	Cohort*time*age²	11.45	.005*
	Genotype	0.92	.351
	CRP	2.77	.108
	QA*cohort	0.63	.435